Transition from a chain-collapse process to a chain-aggregation process of poly(methyl methacrylate) in a mixed solvent

Mitsuo Nakata, Yoshiki Nakamura, and Naoki Sasaki
Department of Polymer Science, Faculty of Science, Hokkaido University, Kita-ku, Sapporo 060-0810, Japan

Yasuyuki Maki
Department of Biological and Chemical Engineering, Faculty of Engineering, Gunma University, Kiryu 376-8515, Japan
(Received 30 April 2007; published 18 October 2007)

The transition from a chain-collapse process to a chain-aggregation process was studied by static light scattering on poly(methyl methacrylate) of the molecular weight $m_w=1.22\times10^7$ in the mixed solvent tert-butyl alcohol+water (2.5 vol %). The concentration c of the solutions ranged from 0.5 to 2.5×10^{-4} g/cm^3 and the measurement was carried out at appropriate time intervals up to the time $t(h)=3250$ after the quench to 35.0 °C which was a few degrees below the phase separation temperature. The molecular weight M_w and mean-square radius of gyration $\langle s^2\rangle_z$ were estimated from each scattering curve determined at the finite concentrations. At the initial stage of 100 h, $\langle s^2\rangle_z$ decreased rapidly with the time t indicating the chain collapse, while at the later stage of 3000 h, $\langle s^2\rangle_z$ increased very slowly indicating the chain aggregation. The chain-collapse process and chain-aggregation process could be analyzed separately, though the two processes overlapped appreciably at the higher concentrations. The former process depended slightly on the concentration, while the latter process showed the exponential growth of $\ln M_w\sim ct$ and $\ln\langle s^2\rangle_z\sim ct$. In the plot of $\ln\langle s^2\rangle_z$ versus $\ln M_w$, the chain-collapse process was depicted by different lines depending on the concentration, while the chain-aggregation process was described by a single straight line. The transition from the former to the latter process occurred distinctly near 200 h after the quench irrespective of the concentration.

DOI: 10.1103/PhysRevE.76.041805 PACS number(s): 61.25.Hq, 82.70.−y

I. INTRODUCTION

When a dilute polymer solution is quenched below the phase-separation temperature, the chain collapse and chain aggregation would occur competitively depending on the polymer concentration. The chain-aggregation process becomes slow with decreasing concentration, while the chain collapse process depends hardly on the concentration. Accordingly, at low concentrations, polymer chains would collapse first and the collapsed chains would aggregate forming clusters of various size. Thus, in a limited range of concentration, a transition from a chain-collapse process to a chain-aggregation process would be observed because of a successive occurrence of the processes. The degree of overlapping of the processes would decrease with decreasing concentration. The above description of the chain behavior below the phase separation temperature seems to be plausible and experiments for chain collapse have been carried out at very low concentrations. However, the transition from a chain-collapse process to a chain-aggregation process has not been measured as a function of the concentration. The purpose of this study is to reveal the transition behavior by an experiment on dilute solutions of poly(methyl methacrylate) (PMMA) in the mixed solvent tert-butyl alcohol+water (2.5 vol %).

In previous studies [1–7], we found that dilute solutions of PMMA quenched below the phase-separation temperature underwent very slow phase separation and remained transparent for long time periods of hours to weeks depending on the molecular weight, concentration and solvent species. Taking advantage of this nature, static light scattering measurements were carried out on the dilute solutions to reveal the chain behavior far below the θ temperature. In order to obtain reliable data of static light scattering, the solutions were set in the concentration range of 0.5×10^{-4} to 6×10^{-4} g/cm^3, and the measurements were carried out with the scattering cell of 18 mm inside diameter. Thermal equilibration in the cell required a blank time of 30 min after the quench. In the concentration range the chain collapse occurred first and the aggregation of collapsed chains developed slowly. However, because of the blank time of the first 30 min after the quench, either chain-collapse process or chain-aggregation process was measured in each experimental run: For PMMA of the molecular weight $m_w=12.2\times10^6$ in isoamyl acetate [1], the chain collapse to equilibrium size required long time periods of a few days, and the chain aggregation did not seem to grow appreciably in an experimentally accessible time. On the other hands, for PMMA of $m_w=2.35\times10^6$ and 4.4×10^6 in isoamyl acetate [2,5], the chain collapse finished in the first 30 min after the quench, and consequently only the chain-aggregation process was measured as a cluster formation of collapsed chains. For PMMA of $m_w=1.57\times10^6$ in the mixed solvent tert-butyl alcohol+water (2.5 vol %) [3,6], the chain collapse was too fast to be observed, and the aggregation of collapsed chains occurred in an experimentally accessible time scale. For PMMA of $m_w=12.2\times10^6$ in this mixed solvent [4], the chain-collapse process was observed for time periods from days to weeks depending on the temperature, and the chain aggregation appeared to be extremely slow.

For a solution of polystyrene with $m_w=8.12\times10^6$ in cyclohexane [8], Chu *et al.* carried out an elaborate experiment of dynamic light scattering. On account of the fast chain aggregation in this solution, they used a very dilute solution

of $c=8.7\times10^{-6}$ g/cm^3 and a capillary-tube cell with a wall thickness of 0.01 mm and a diameter of 5 mm to obtain rapid thermal equilibration. The chain collapse seemed to finish within about 10 min after the quench. The chain aggregation was not appreciable during the time and began to grow 12 min after the quench. Thus, the chain-collapse and chain-aggregation processes of polystyrene in cyclohexane occurred rapidly at a short time interval even at the very low concentration, which made a precise study of the processes difficult.

In this study, a successive occurrence of a chain-collapse process and a chain-aggregation process was observed for dilute solutions of PMMA with $m_w=1.22\times10^7$ by static light scattering which was carried out for a time period of 3250 h (19 weeks). The chain-collapse process finished at the initial stage of 200 h after the quench, while the chain aggregation developed very slowly and became observable at the later stage of 3000 h. The chain-collapse process and the chain-aggregation process appeared to occur independently because of the very different time scales of the processes. In the last part of Sec. IV, a brief discussion on the mechanism of the slow chain aggregation was made in terms of the two characteristic times of contact and interdiffusion [9–11]. The rates of chain collapse and chain aggregation were conjectured to have the same molecular weight dependence.

II. EXPERIMENTAL AND DATA ANALYSES

The light-scattering measurement was carried out on solutions of a PMMA fraction in the mixed solvent tert-butyl alcohol+water (2.5 vol %) after the quench to 35.0 °C from the θ temperature 41.5 °C. The scattering data were obtained at an angular interval of 15° in the range from 30° to 150° with unpolarized incident light at 435.8 nm of a mercury arc as described elsewhere [4]. The PMMA fraction M21-F9 used in this study was characterized as the weight-average molecular weight $m_w=1.22\times10^7$, the characteristic ratio $\langle s^2\rangle_o/m_w=6.7\times10^{-18}$cm^2 and the molecular weight distribution $m_w/m_n\sim1.2$ previously [4]. A stock solution was prepared and diluted in scattering cells of 18 mm inside diameter to the concentrations of c (10^{-4} g/cm^3)=0.596, 1.247, 1.843, and 2.489. Each cell was sealed tightly by a Teflon cap to prevent evaporation of the solvent and stored in a glass tube partially filled with the solvent. The glass tube was immersed in a water bath controlled at 41.5 °C. The light scattering apparatus was equipped with an optical cylindrical cell, which was filled with the solvent and controlled at 35.0 °C. Each scattering cell was transferred into the cylindrical cell from the glass tube, subjected to intensity measurements 30 min later for thermal equilibration and backed to another glass tube controlled at 35.0 °C. This measurement was carried out for the four solutions successively and repeated at appropriate time intervals for the time period of 19 weeks keeping the solutions at 35.0 °C. The refractive index increment was estimated to be $dn/dc=0.111$ at 35.0 °C [4].

The light scattering data were obtained as a function of the scattering angle θ and the concentration c. The scattered intensity at an angle θ was transformed to the excess Rayleigh ratio R_θ from polymer and analyzed by the scattering equation [12]

$$(Kc/R_\theta)^{1/x}=M_w^{-1/x}\{1+(1/3x)\langle s^2\rangle_z q^2+(2/x)M_wA_2c\} \quad (1)$$

with $K=(2\pi^2n^2/N_A\lambda^4)(dn/dc)^2$ and $q=(4\pi n/\lambda)\sin(\theta/2)$, where N_A is Avogadro's number, λ is the wavelength of incident light in a vacuum, and n is the refractive index of the solution. M_w, $\langle s^2\rangle_z$ and A_2 represent the weight-average molecular weight, z-average mean-square radius of gyration, and the second virial coefficient for dilute polymer solutions, respectively. The constant x should be chosen in such a way as the plot of $(Kc/R_\theta)^{1/x}$ vs $\sin^2(\theta/2)$ may be linear in a wide angular range. In the present study, we used the value $x=1.5$, which had been shown to be suitable to analyses of light-scattering data for large molecular weight [4,12].

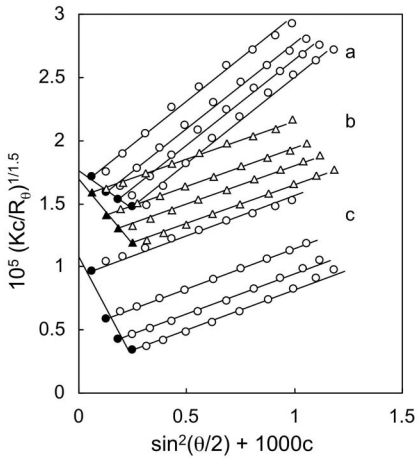

FIG. 1. Time evolution of scattered intensities from poly(methyl methacrylate) (PMMA) with $m_w=1.22\times10^7$ in the mixed solvent tert-butyl alcohol+water (2.5 vol %) in a form of the Zimm plot due to Eq. (1). The plots (a), (b), and (c) were obtained 2, 109, and 2329 h after the quench from the θ temperature 41.5 to 35.0 °C.

Figure 1 gives a time evolution of scattered intensities by using the Zimm plot due to Eq. (1) with $x=1.5$. The plots a, b, and c were obtained at 2, 109, and 2329 h (14 weeks) after the quench to 35.0 °C. In each plot, the points for angular dependence are represented by parallel straight lines and extrapolated to $\theta=0$ as indicated by the filled symbols, which are described by the straight line and extrapolated to $c=0$. The Zimm plots at 2 h, 109 and 2329 yield the molecular weight $M_w\times10^{-7}=1.35$, 1.41, and 2.24, the second virial coefficient $A_2\times10^5=-4.7$ cm^{3}mol/g^2, −7.2, and −12.7, and the mean-square radius of gyration $\langle s^2\rangle_z\times10^{-3}=2.34$, 1.03, and 1.17 nm^2, respectively. In the process between 2 h and 109 after the quench, M_w increases slightly, while $\langle s^2\rangle_z$ decreases remarkably. This means a chain-collapse process. The large value of M_w obtained at 2329 h can be attributed to a chain aggregation, and consequently the Zimm plot c is not significant for an analysis of the data, though the plot c is similar to the plot b in appearance. A close inspection of the plot c indicates that the slope of the plot of $(Kc/R_\theta)^{1/1.5}$ vs $\sin^2(\theta/2)$ increases with increasing concentration. Thus, in addition to the analysis by the Zimm plot, it is necessary to

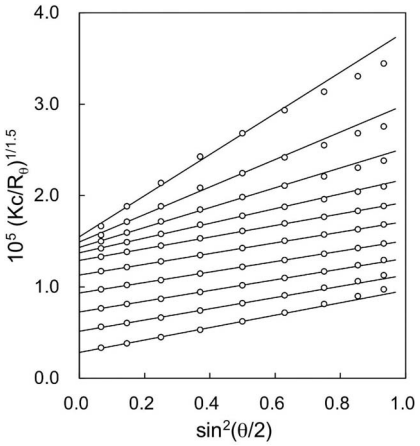

FIG. 2. Time evolution of scattered intensities from PMMA with $m_w=1.22\times10^7$ in the mixed solvent at $c=1.843\times10^{-4}$ g/cm^3 by the plot due to Eq. (1). The plots from the top to the bottom were obtained 0.5, 2, 7, 29, 109, 313, 649, 1129, 1849, and 3250 h after the quench to 35.0 °C.

estimate M_w and $\langle s^2\rangle_z$ from each scattering curve at the finite concentrations in order to disclose the transition from the chain-collapse to the chain-aggregation process.

Figure 2 shows the plot of $(Kc/R_\theta)^{1/1.5}$ vs $\sin^2(\theta/2)$ for the solution at $c=1.843\times10^{-4}$ g/cm^3 at the time 0.5, 2, 7, 29, 109, 313, 649, 1129, 1849, and 3250 h from the top to the bottom. The straight lines were obtained by a least-squares method for data points in the angular range from 30° to 105° on account of the slightly curved character. The intercept and slope of the straight lines were analyzed by using Eq. (1) without the term due to A_2 to estimate M_w and $\langle s^2\rangle_z$.

The phase separation temperatures of the present solutions were predicted to exist between 37.0 and 39.0 °C. After the chain-collapse process finished, scattered intensities from the solutions remained constant at 39.0 °C but increased steadily at 37 °C. However, an accurate determination of the phase separation temperature was unfeasible because of the extremely slow phase separation. For solutions of PMMA of the lower molecular weights $m_w\times10^{-6}=1.57$, 2.84, and 4.0, the phase separation temperature has been measured carefully [4]. These measurements made by changing m_w support the above prediction for the present solutions.

III. TRANSITION FROM CHAIN-COLLAPSE PROCESS TO CHAIN-AGGREGATION PROCESS

Figure 3 shows a time evolution of M_w by the plot of $\ln M_w$ versus the time t (h). The symbols of diamond, square, triangle, and circle represent data of the solutions at $c(10^{-4}$ g/cm$^3)=0.596$, 1.247, 1.843, and 2.489, respectively. The crosses represent values extrapolated to $c=0$ by using the Zimm plot. Since the extrapolated point at $t=1849$ h yields a large molecular weight as $M_w=1.93\times10^7$, the analysis of single polymer chains by the Zimm plot is not made properly. The straight lines are fitted to points in the range from 385 to 1225 h. The slope of the line increases with increasing concentration indicating a characteristic of

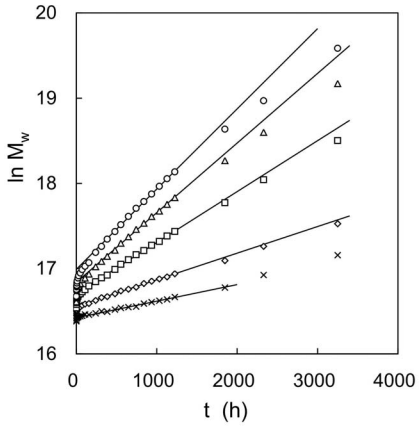

FIG. 3. Time evolution of the molecular weight M_w of PMMA in the mixed solvent tert-butyl alcohol+water (2.5 vol %) after the quench to 35.0 °C. The plots of $\ln M_w$ versus the time t (h) were obtained at the concentration c (10^{-4} g/cm^3)=0 (cross), 0.596 (diamond), 1.247 (square), 1.843 (triangle), and 2.489 (circle). The values at $c=0$ were obtained by extrapolating scattered intensities to $c=0$ by means of the Zimm plot. The straight lines were fitted to the data in the range from 385 to 1225 h.

chain aggregation. A deviation from the straight line is seen at the initial stage and at large $\ln M_w$. Figure 4 shows a plot of $\ln M_w$ versus t at small t in an enlarged scale with the same symbols and the same straight lines as those in Fig. 3. The deviation of the data points from the straight lines diminishes with decreasing concentration and vanishes at the limit of $c=0$. This behavior of M_w could be attributed to the data analysis by Eq. (1) without the term due to A_2 and would be an apparent one as seen later.

Figure 5 shows a semilogarithmic plot of $\langle s^2\rangle_z$ (nm^2) versus the time t (h) with the same symbols as in Fig. 3. The straight lines are fitted to data points in the range from 385 to 1225 h. Figure 6 shows the initial behavior in an enlarged scale with the same symbols and the same lines as in

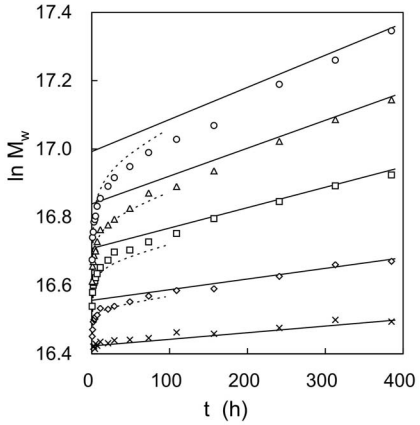

FIG. 4. Time evolution of $\ln M_w$ at small time t (h) in an enlarged scale. The symbols and the straight lines are the same as those in Fig. 3. The dotted lines give R_θ/Kc at $\theta=0$ estimated by using Eq. (1) with the experimental values of M_w and A_2 due to the Zimm plot.

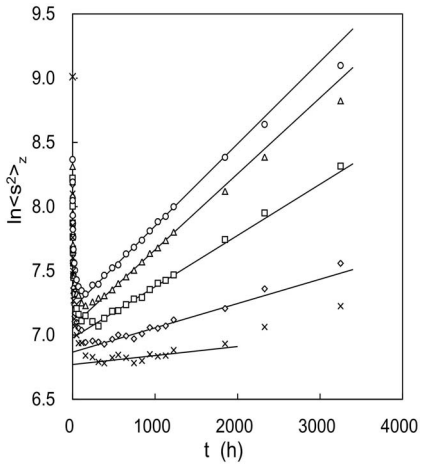

FIG. 5. Time evolution of the mean square radius of gyration $\langle s^2\rangle_z$ (nm^2) of PMMA in the mixed solvent after the quench to 35.0 °C. The plots of ln $\langle s^2\rangle_z$ versus the time t (h) were obtained at the concentration c (10^{-4} g/cm^3)=0 (cross), 0.596 (diamond), 1.247 (square), 1.843 (triangle), and 2.489 (circle). The values at c=0 were obtained by extrapolating scattered intensities to c=0 by means of the Zimm plot. The straight lines were fitted to the data in the range from 385 to 1225 h. The star on the ordinate indicates the data obtained at the θ temperature.

Fig. 5. The plots in Figs. 5 and 6 reveal two different processes distinctly. At the initial stage $\ln\langle s^2\rangle_z$ decreases rapidly with t due to chain collapse, while at the later stage $\ln\langle s^2\rangle_z$ increases linearly with t due to chain aggregation. This behavior at the later stage is in accord with the behavior of ln M_w in Fig. 3. In Fig. 6 the chain-collapse process tends to overlap with the chain-aggregation process at the higher concentrations, while at the lower concentrations the chain collapse appears to finish before the chain aggregation becomes perceptible. Since at the limit of c=0 the chain aggregation would vanish, M_w should be constant and $\langle s^2\rangle_z$ should approach a constant value for single globules at large t. However, each straight line at c=0 in Figs. 3 and 5 has a slight slope, which is attributed to the improper extrapolation to c =0 from the high concentrations in the Zimm plot. Since the

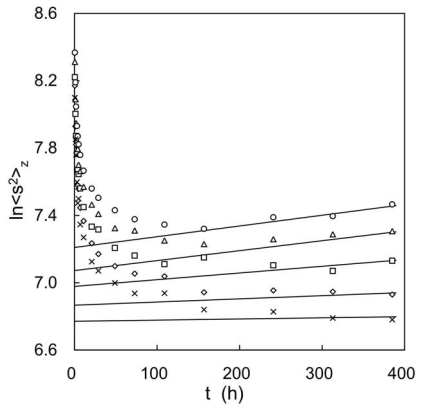

FIG. 6. Time evolution of $\ln\langle s^2\rangle_z$ at small time t (h) in an enlarged scale. The symbols and the straight lines are as in Fig. 5.

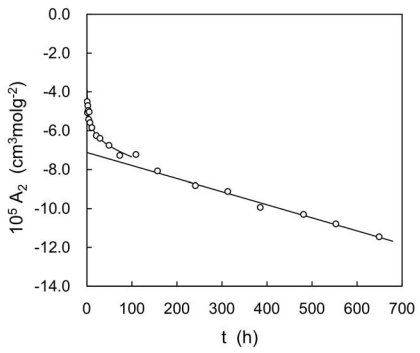

FIG. 7. Time evolution of the second virial coefficient A_2 cm^3 mol/g^2 estimated with the Zimm plot. The straight line is fitted to the data point in the range of 157 to 649 h. The solid curve is described by Eq. (7).

chain collapse appears to finish rapidly in Fig. 6, the straight lines fitted to the data points in the range from 385 to 1225 h would represent the chain aggregation process accurately.

The analysis by the Zimm plot due to Eq. (1) gives the second virial coefficient A_2. Figure 7 shows the plot of A_2 (cm^{3}mol/g^2) versus t (h). A_2 at the initial stage decreases rapidly with t. At the later stage A_2 decreases linearly with t as shown by the straight line, which is fitted to data points in the range from 157 h to 649. The rapid decrease of A_2 at the initial stage is caused by the chain collapse, because the interaction between polymer chains would change with the size of the chains. The steady decrease of A_2 at the later stage is ascribed to the chain aggregation.

Figure 8 shows the plot of $\ln\langle s^2\rangle_z$ versus ln M_w with the same symbols as in Fig. 3. The data extrapolated to c=0 are omitted. The chain-collapse process behaves differently depending on the concentration, while the chain-aggregation process is represented by a single straight line irrespective of the concentration. The data points for large clusters which deviate from the straight lines in Figs. 3 and 5 also fall on the single straight line. In Fig. 8 the transition from the chain collapse to the chain aggregation appears to occur sharply

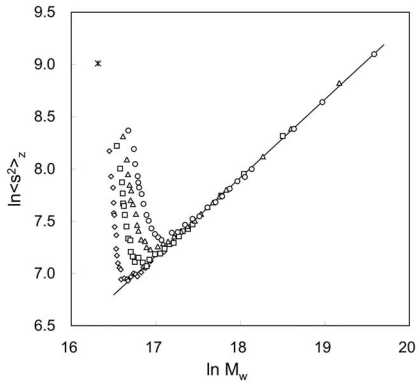

FIG. 8. Double logarithmic plot of $\langle s^2\rangle_z$ versus M_w for PMMA in the mixed solvent after the quench to 35.0 °C. The symbols of the points are as in Fig. 3. Data points at c=0 is omitted. The star indicates the data of single chains at the θ temperature. The straight line is fitted to data in the range of 313 to 3250 h.

TABLE I. Values of the parameters in Eqs. (2), (3), and (5).

c (10^{-4} g/cm^3)	G (10^{-4} h^{-1})	H (10^{-4} h^{-1})	M_{wg} (10^7 g/mol)	$\langle s^2\rangle_{zg}$ (10^3 nm^2)	β	τ_s (h)
0[a]			1.36	0.87	0.233	0.209
0.596	3.12	1.89	1.55	0.96	0.238	0.267
1.247	5.97	3.99	1.81	1.07	0.242	0.330
1.843	8.17	5.92	2.06	1.18	0.246	0.442
2.489	9.41	6.40	2.40	1.35	0.275	0.663

[a]Obtained by extrapolating light scattering data to zero concentration on the Zimm diagram.

near points at the time $t=241$ h irrespective of the concentrations, though the points are not indicated explicitly. Correspondingly, the data points in Figs. 4 and 6 come close to the straight lines near $t=241$ h. The straight line in Fig. 8, which is fitted to data points in the range $t>300$ h, gives the relation $\langle s^2\rangle_z = AM_w^{2/D}$ with $D=2.67$ and $A=3.83\times10^{-3}$.

IV. DISCUSSION

In previous studies [2,3,5,6], the light scattering data for chain aggregation were analyzed by the Guinier plot of $\ln(R_\theta/Kc)$ versus $\sin^2(\theta/2)$ for spherical particles. The plot for large clusters at a later stage was curved considerably and the estimation of $\langle s^2\rangle_z$ was not made accurately. The plots in Fig. 2 are well represented by the straight lines irrespective of the state of polymer chains and therefore are useful to estimate M_w and $\langle s^2\rangle_z$ for contracted chains, compact globules, and clusters of polymer chains in a consistent way. However, the straight lines at the later stage in Fig. 2 do not necessarily imply a similar structure for collapsed chains and for chain clusters because of the increasing size distribution of clusters with the time.

The straight lines in Figs. 3 and 5 can be expressed, respectively, by

$$\ln M_{wa} = \ln M_{wg} + Gt, \tag{2}$$

$$\ln\langle s^2\rangle_{za} = \ln\langle s^2\rangle_{zg} + Ht, \tag{3}$$

where $\ln M_{wg}$ and $\ln\langle s^2\rangle_{zg}$ are the intercepts at $t=0$, and G and H are the slops of the plots. The suffix a of M_{wa} and $\langle s^2\rangle_{za}$ is attached to denote chain aggregation. The parameters in Eqs. (2) and (3) were estimated from the straight lines in Figs. 3 and 5, respectively, as listed in Table I. The values of M_{wg} and $\langle s^2\rangle_{zg}$ at the finite concentrations would be interpreted as due to dissociated equilibrium globules, though the values are estimated from the data of chain-aggregation process. M_{wg} and $\langle s^2\rangle_{zg}$ at $c=0$ would represent the molecular weight and mean-square radius of gyration of equilibrium single globules, respectively.

The chain-collapse process of single chains has been described by a stretched exponential function [4,7]. The mean-square radius of gyration $\langle s^2\rangle_{zc}$ in the chain-collapse process at the finite concentrations shown in Fig. 6 would be also expressed by the stretched exponential function as

$$\langle s^2\rangle_{zc} = \langle s^2\rangle_{zg} + (\langle s^2\rangle_{z\theta} - \langle s^2\rangle_{zg})\exp[-(t/\tau_s)^\beta], \tag{4}$$

where β and τ_s are constant independent of the time t. $\langle s^2\rangle_{z\theta}$ would be given by the unperturbed radius of gyration obtained at the θ temperature and independent of the concentration. $\langle s^2\rangle_{zc}$ would depend on the concentration through $\langle s^2\rangle_{zg}$, β, and τ_s. The behavior of $\langle s^2\rangle_z$ shown in Fig. 5 could be represented by combining Eqs. (3) and (4) as

$$\langle s^2\rangle_z = \langle s^2\rangle_{za} + (\langle s^2\rangle_{z\theta} - \langle s^2\rangle_{zg})\exp[-(t/\tau_s)^\beta]. \tag{5}$$

Since the first term on the right hand is given by Eq. (3), the parameters β and τ_s could be determined by the plot of $\ln\{\ln[(\langle s^2\rangle_{z\theta}-\langle s^2\rangle_{zg})/(\langle s^2\rangle_z-\langle s^2\rangle_{za})]\}$ versus $\ln t$. The plots were linear and the parameters were determined as shown in Table I. According to this analysis, β and τ_s depend significantly on the concentration. However, the dependence of the chain-collapse process on the concentration is not so large as affect the behavior of the Zimm plots in Fig. 1. Figure 9 exhibits the plot of $\langle s^2\rangle_z$ versus $\ln t$ with the same symbols as in Fig. 5. Two data points at the last time 3250 h are beyond the scale of the plot. The solid curves, which are described by Eq. (5) with the values of the parameters in Table I, agree with the data points reasonably. At the higher concentrations, the chain-collapse process and chain-aggregation process appear to overlap with each other. The separation between the

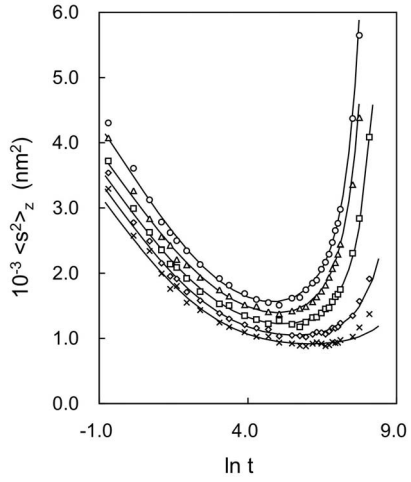

FIG. 9. Transition from chain collapse to chain aggregation by the plot of $\langle s^2\rangle_z$ versus $\ln t$ with t in h. The symbols of the points are as in Fig. 3. The solid lines are described by Eq. (5).

two processes becomes clear with decreasing concentration. At the limit of $c=0$, $\langle s^2\rangle_z$ varies slightly between 918 and 930 nm^2 in the wide range of 200 to 800 h. Thus, the flat minimum corresponds to an asymptotic behavior of chain collapse and indicates an equilibrium globule of $\langle s^2\rangle_z = 920$ nm^2, which can be compared with $\langle s^2\rangle_{zg}=870$ nm^2 at $c=0$ in Table I and also with 970 nm^2 obtained previously [4]. The plots in Fig. 9 unveil the chain behavior below the phase separation temperature and would legitimate the determination of the size of single globules by light scattering measurements at the low concentrations [1,4,7].

It is interesting to look into the relation between the apparent behavior of M_w in Fig. 4 and the time dependence of A_2 in Fig. 7. The second virial coefficient A_{2c} in the chain-collapse process would be consist of the two part: one is caused directly by the temperature change, and the other is caused by the chain collapse and depend on the time. By analogy with the behavior of $\langle s^2\rangle_{zc}$, A_{2c} was assumed to be written as

$$A_{2c} = A_{2g} + (A_{20} - A_{2g})\exp[-(t/\tau_v)^\gamma], \tag{6}$$

where γ and τ_v are constants independent of t. A_{2g} is the second virial coefficient for fully collapsed chains and A_{20} is caused by the temperature change due to the sudden quench. The behavior of A_2 in Fig. 7 could be written as

$$A_2 = B + (A_{20} - A_{2g})\exp[-(t/\tau_v)^\gamma], \tag{7}$$

where B would be given by the straight line in Fig. 7 and can be written as $B=A_{2g}-bt$. Since the present purpose is to demonstrate a correlation between M_w and A_2, we tentatively assumed $A_{20}=0$. With $A_{2g}=-7.1\times10^{-5}$ and $b=-6.7\times10^{-8}$ estimated from the straight line, γ and τ_v were determined by the plot of $\ln\{\ln[(A_{20}-A_{2g})/(A_2-B)]\}$ versus $\ln t$ as $\gamma=0.239$ and $\tau_v=1.38$. The solid curve at small t in Fig. 7 was depicted by Eq. (7) with these values. The behavior of M_w in Fig. 4 was calculated as shown by the dotted lines by using the relation $M_w=R_0/Kc$, where R_0/Kc was given by Eq. (1) with the experimental values of A_2 due to Eq. (7) and M_w at $c=0$. The agreement between the dotted lines and the data points indicates that the apparent behavior of M_w is caused by the interaction between chains. Thus, the straight lines in Figs. 3 and 4 represent the chain aggregation of fully collapsed chains. In previous studies [2,3,5,6], the apparent behavior of M_w was not observed because of the fast chain collapse: The measurements for chain aggregation were carried out after a completion of chain collapse.

The stars in Fig. 8 and on the ordinate in Fig. 5 represent the data of the unperturbed radius of gyration $\langle s^2\rangle_{z\theta}=8.2\times10^3$ nm^2 and $m_w=1.22\times10^7$ obtained at θ temperature. It is seen that this radius is larger than those of clusters in the chain-aggregation process. The last measurement at $t=3250$ h gives $M_w=4.1\times10^7$ and $\langle s^2\rangle_z=1.92\times10^3$ nm^2 at $c=0.596\times10^{-4}$ g/cm^3, and $M_w=3.2\times10^8$ and $\langle s^2\rangle_z=8.9\times10^3$ nm^2 at $c=2.489\times10^{-4}$ g/cm^3. The latter $\langle s^2\rangle_z$ is comparable with $\langle s^2\rangle_{z\theta}$, and M_w is about 30 times of m_w for single chains. The former $\langle s^2\rangle_z$ is about a quarter of $\langle s^2\rangle_{z\theta}$ and M_w is only three times of m_w, that is, trimers are formed on average even at $t=3250$ h. The transition from chain collapse to chain aggregation shown in Fig. 8 is found to occur in a very narrow range of M_w by taking the values of $\ln M_w=16.3$ for monomer and 17.0 for dimer into account. This means that the phase separation would occur by forming clusters of various size as dimer, trimer, and so on without a critical nucleus. This kind of phase separation has been predicted to occur below the coil-globule transition temperature, where the concentration in a single globule is comparable with that of the concentrated phase and each globule may act as a critical nucleus [13]. It should be mentioned that the points given by M_{wg} and $\langle s^2\rangle_{zg}$ in Table I were located in close vicinity to the straight line in Fig. 8. Accordingly, the single globules would have characteristics similar to those of clusters in the chain-aggregation process. Furthermore, it was predicted that above the coil-globule transition temperature a small cluster of which the number of chains is less than ten may have a size smaller than that of a single chain at the same temperature [13,14]. The behavior of the plots in Figs. 8 and 9 does not indicate an existence of clusters of smaller sizes than that of the single globule. For the present system the coil-globule transition temperature T_{cg} has been estimated as $(1-\theta/T_{cg})m_w^{1/2}=39.2$ [4], which gives $T_{cg}=39.6$ °C for $m_w=1.22\times10^7$. Thus, the result of the present experiment carried out at 35 °C is not incompatible with the theoretical prediction.

In previous studies, the chain aggregation process below the coil-globule transition temperature was investigated for PMMA of $m_w=1.57\times10^6$ in tert-butyl alcohol+water (2.5 vol %) [3,6] and PMMA of $m_w=2.35\times10^6$ and 4.4×10^6 in isoamyl acetate [2,5]. The chain collapse in the solutions finished in the blank time of the first 30 min after the quench, and both M_w and $\langle s^2\rangle_z$ were observed to increase from the values of dissociated single globules. Thus, the phase separation occurred without forming a critical nucleus. The logarithmic plot of M_w versus $\langle s^2\rangle_z$ for the chain-aggregation process yielded a single straight line. For PMMA of $m_w=1.57\times10^6$ in the mixed solvent, the exponent D in $\langle s^2\rangle_z \sim M_w^{2/D}$ has been estimated as 2.53 at 25.0 °C and 2.66 at 30.0 °C [3], which are comparable with the present one for $m_w=1.22\times10^7$. The behavior of the chain-aggregation process in the mixed solvent does not seem to change markedly with the molecular weight, though the rate of the process depends largely on the molecular weight.

In Fig. 10, the coefficients G in Eq. (2) and H in Eq. (3) are plotted against the concentration c. Both the plots of G (circles) and H (triangles) are represented by the straight lines passing through the origin except for the points at the highest concentration. It is not certain whether this deviation is due to a solution condition or genuine characteristics at higher concentrations. According to our experience, chain-aggregation behavior of a dilute polymer solution was sometimes affected by a subtle change of the solution condition caused in the preparation process. In Fig. 10, at least at the low concentration the coefficients G and H can be put as

$$G = gc, \tag{8}$$

$$H = hc, \tag{9}$$

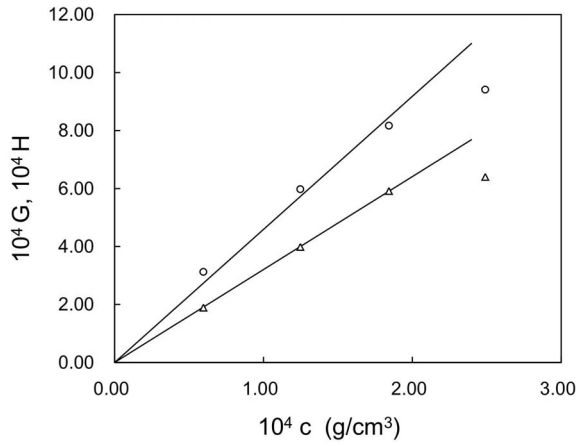

FIG. 10. Rates $G(h^{-1})$ and $H(h^{-1})$ of chain aggregation as a function of the concentration c. The circles and triangles are for G and H due to M_w and $\langle s^2\rangle_z$, respectively. The straight lines give $g=4.59$ (cm^3/gh) and $h=3.20$ in Eqs. (8) and (9), respectively.

where g and h represent the specific rates of chain aggregation. The plots in Fig. 10 give $g=4.59$ (cm^3/gh) and $h=3.20$. These values are not independent of each other because of the relation $g/h=D/2$ due to $\langle s^2\rangle_z=AM_w^{2/D}$.

In previous studies, the values of g and h were determined for PMMA in the mixed solvent as $g=2.09\times10^3$ (cm^3/gh) and $h=1.50\times10^3$ for $m_w=1.57\times10^6$ at 33.0 °C [6], and for PMMA in isoamyl acetate as $g=3.13\times10^3$ (cm^3/gh) and $h=2.15\times10^3$ for $m_w=2.35\times10^6$ at 25.0 °C [2], and as $g=7.0\times10^2$ (cm^3/gh) and $h=4.5\times10^2$ for $m_w=4.4\times10^6$ at 30.0 °C [5]. The values of g and h obtained in the present study are much smaller than these values obtained in the previous studies. At present the specific rate appears to depend on the solvent unexpectedly and cannot be correlated to characteristics of the solvent. On the other hand, it is possible to see the molecular weight dependence of the specific rate. The dependence was assumed as $g\sim m_w^{-\mu}$. Then, the above experimental values of the specific rates for PMMA in the mixed solvent and in isoamyl acetate give $\mu=3.0$ and 2.4, respectively. The values of μ estimated from g and h agreed with each other within an experimental error. The rate of chain aggregation has been found to depend on temperature considerably [3]. The molecular weight difference should be large in order to determine μ accurately. Thus, the value of $\mu=3.0$ in the mixed solvent seems to be more reliable than that in isoamyl acetate.

The slow growths of M_w and $\langle s^2\rangle_z$ and the exponential relations of Eqs. (2) and (3) are characteristics of the reaction limited cluster aggregation (RLCA) [15]. As for the Smoluchowski equation [16], RLCA is described with the collision kernel $K_{ij}=B(i+j)$ for a collision of i-mer and j-mer with B being a constant, and the characteristic time is derived as $\tau_{sr}=m/2Bc$ with m being the molecular weight of monomer [5]. Equations (2) and (8) give the characteristic time $\tau_{\mathrm{exp}}=1/gc$ and suggest the molecular weight dependence of $B\sim m^{1-\mu}$. The Smoluchowski equation for RLCA could be used to estimate a time evolution of the cluster size distribution from the observed chain aggregation process [5,6]. However, the phenomenological analysis is not concerned with the mechanism of RLCA. A different point of view is necessary to inquire the mechanism. In RLCA only a small fraction of collisions between two clusters yields a coalescence of the clusters. When chains can migrate between two clusters by diffusion during a contact, a coalescence of the clusters could occur. This idea can be represented with the two characteristic times, that is, the chain diffusion time τ_r and contact time τ_c [9,10]. For $\tau_r/\tau_c\gg1$ chains could hardly bridge two clusters during a contact and the aggregation would occur due to RLCA. For $\tau_r/\tau_c\ll1$ the aggregation would be due to the diffusion limited cluster aggregation (DLCA), because each collision of two clusters would give rise to a coalescence of them. The Smoluchowski equation was derived originally for DLCA and gave the characteristic time $\tau_{sd}=3\eta m/4N_AkTc$, where k is the Boltzmann constant and η is the viscosity of the solvent [16]. For the present solution at $c=2.5\times10^{-4}$ g/cm^3, τ_{sd} can be estimated to be 10^{-2} s, which is several orders of magnitude smaller than the experimental time scale.

Tanaka observed an anomalous phase separation for poly(vinyl methyl ether) in water [9]. In a restricted region of concentration and temperature, small droplets were observed to move around vigorously by phase-contrast microscopy. The droplets did not undergo coalescence and seemed to be stable. In order to explain this phenomenon he calculated τ_r and τ_c roughly and showed that τ_r is several orders of magnitude longer than τ_c. The estimation of τ_r was made with a reptation time $a^2N^3\phi^{3/2}/D_1$ for a polymer in a dense polymer matrix [17], and an upper limit of τ_c was estimated by r_0^2/D_R due to Brownian motion of droplet with radius R, where a is the length of a chain segment, N is the number of segment in a chain, ϕ is the volume fraction of polymer in a droplet, D_1 and D_R are the diffusion constants of a segment and a droplet, respectively, and r_0 is the range of interaction. The large value obtained for τ_r/τ_c was compatible with the observed stable droplet. The estimation of τ_r/τ_c could be also made for the present chain aggregation process. Both the interaction range and the radius of a cluster were assumed to be equal to $\langle s^2\rangle_z^{1/2}$, i.e., $r_0=R=\langle s^2\rangle_z^{1/2}$, though r_0 appeared to be much smaller than R. This assumption yields $\tau_c=9\times10^{-5}p^{1.12}$ (s) with the relation $\langle s^2\rangle_z=AM_w^{2/D}$ and the average number of chains $p=M_w/1.22\times10^7$ in a cluster. The volume fraction of polymer in a cluster is expressed as $\phi=0.086p^{-0.12}$ and τ_r is obtained as $\tau_r=5\times10^4p^{-0.19}$ (s) for $N=1.22\times10^5$ and $a=0.61$ nm [2]. Thus, τ_r/τ_c is roughly 10^8 for $p=1$ and 10^6 for $p=30$. In the case of $\tau_r/\tau_c\gg1$ the aggregation behavior may be dominated by τ_r. It is interesting to observe that τ_r given above depends on the molecular weight m of polymer as $\sim m^3$, which is compatible with the observed rate of chain aggregation of $g\sim m_w^{-\mu}$ with $\mu=3.0$. However, it should be noticed that the above expression of τ_r is derived for reptation of a polymer chain in a dense polymer matrix, while the present clusters contains a small number of chains; g was estimated in the range $\ln M_w<18$ which corresponds to $p<6$. Chuang *et al.* argued a RLCA of polymer chains in a different way [11]. They demonstrated an existence of an entanglement force acting between two approaching polymer globules in poor solvent by a molecular

dynamic simulation. This force was shown to be strong enough to slow down the aggregation of polymer globules indicating $\tau_r/\tau_c \gg 1$. This argument for two approaching polymer globules is suggestive to the present slow formation of small clusters, though the molecular weight dependence of the force is not investigated.

Theoretical studies on the kinetics of chain collapse were carried out with a phenomenological model and proposed a two-stage collapse process [18,19]. At the first stage polymer chains collapse to crumpled globules in a self-similar manner, and at the second stage the crumpled globules contract to equilibrium globules by a reptationlike motion. The characteristic times of chain collapse at the first and second stages were predicted to depend on the molecular weight as m^2 and m^3, respectively. It has been argued that the characteristic times due to the theories are by several orders of magnitude smaller than experimental time scales of chain collapse of PMMA and polystyrene [1,8]. On the other hand, according to our recent experimental study on PMMA solutions [20], the characteristic time of chain collapse depends on the molecular weight as m^3, which is in accord with the theoretical prediction at the second stage. It should be noticed that this molecular weight dependence is the same as that of chain aggregation.

As mentioned in Sec. I, it is seen for PMMA solutions that the chain-collapse process finishes before the chain-aggregation process becomes noticeable. This phenomenon was observed irrespective of the molecular weight, which could be explained by the characteristic times of the processes having the same molecular weight dependence. In the present study on the PMMA solution with $m=1.22\times10^7$, a successive occurrence of the chain-collapse and chain-aggregation processes was measured by an experiment carried out for a long time period of 19 weeks. The transition from the former to the latter process was represented by a superposition of the two processes, though the overlapping of the processes became noticeable at higher concentrations. In view of the same molecular weight dependences of the characteristic times of m^3, the transition behavior in a solution of a different molecular weight would occur similarly in a different time scale. Because of the rapid change of the characteristic times with the molecular weight, a measurement of the transition could be permitted for the solution of a molecular weight in a restricted range.

[1] M. Nakata and T. Nakagawa, J. Chem. Phys. **110**, 2703 (1999).
[2] M. Nakata, T. Nakagawa, Y. Nakamura, and S. Wakatsuki, J. Chem. Phys. **110**, 2711 (1999).
[3] Y. Nakamura, T. Nakagawa, N. Sasaki, A. Yamagishi, and M. Nakata, Macromolecules **34**, 5984 (2001).
[4] Y. Nakamura, N. Sasaki, and M. Nakata, Macromolecules **34**, 5992 (2001).
[5] T. Nakagawa, Y. Nakamura, N. Sasaki, and M. Nakata, Phys. Rev. E **63**, 031803 (2001).
[6] Y. Nakamura, N. Sasaki, and M. Nakata, Macromolecules **35**, 1365 (2002).
[7] Y. Maki, N. Sasaki, and M. Nakata, Macromolecules **37**, 5703 (2004).
[8] B. Chu, Q. Ying, and A. Yu. Grosberg, Macromolecules **28**, 180 (1995).
[9] H. Tanaka, Macromolecules **25**, 6377 (1992).
[10] H. Tanaka, J. Chem. Phys. **100**, 5323 (1994).
[11] J. Chuang, A. Yu. Grosberg, and T. Tanaka, J. Chem. Phys. **112**, 6434 (2000).
[12] M. Nakata, Polymer **38**, 9 (1997).
[13] G. Raos and G. Allegra, J. Chem. Phys. **107**, 6479 (1997).
[14] G. Raos and G. Allegra, Macromolecules **29**, 8565 (1996).
[15] T. Vicsek, *Fractal Growth Phenomena*, 2nd ed. (Word Scientific, Singapore, 1992).
[16] M. von Smoluchowski, Z. Phys. Chem. **92**, 129 (1917).
[17] P. G. de. Gennes, *Scaling Concepts in Polymer Physics* (Cornell University Press, New York, 1979).
[18] P. G. de Gennes, J. Phys. (France) Lett. **46**, L639 (1985).
[19] A. Yu. Grosberg, S. K. Nechaev, and E. I. Shakhnovich, J. Phys. (France) **49**, 2095 (1988).
[20] Y. Maki, T. Dobashi, and M. Nakata, J. Chem. Phys. **126**, 134901 (2007).